Chemical Engineering Journal 94 (2003) 93–98

Chemical Engineering Journal

www.elsevier.com/locate/cej

The active phase distribution in Ni/Al_2O_3 catalysts and mathematical modeling of the impregnation process

E.M. Assaf [a,*], L.C. Jesus [b], J.M. Assaf [b]

[a] *Departamento de Físico-Química, Instituto de Química de São Carlos, Universidade de São Paulo, Av. Trabalhador Sãocarlense, 400 São Carlos, SP 13560-970, Brazil*

[b] *Departamento de Engenharia Química, Universidade Federal de São Carlos, Rod. W. Luiz, km 235, São Carlos, SP, Brazil*

Received 5 November 2002; accepted 13 December 2002

Abstract

This paper deals with the formation of nickel distribution profiles in NiO/Al_2O_3 catalysts prepared by dry impregnation of spherical pellets of γ-alumina with nickel nitrate aqueous solutions. The experimental concentration profiles were obtained and a mathematical model for the impregnation process was proposed and used to identify the main process parameters. The partial-differential equations of the model that describe the nickel concentration profiles and the fractional coverage were numerically solved. Backward finite-difference formulas were used to discretize the space variable and the resulting set of ordinary-differential equations was integrated with respect to time using a marching algorithm. The impregnation conditions determine the distribution of the active phase along the pellet. The concentration of the impregnation solution and the time of contact were important in the definition of the profiles, while the effect of the impregnation temperature was less significant. Satisfactory agreement was achieved between model predictions and experimental data, revealing that the simplifications assumed in the model are sound under the experimental conditions studied.

Keywords: Impregnation process; Nickel concentration profiles; Ni/Al_2O_3 catalysts; Mathematical modeling

1. Introduction

In the preparation of supported catalysts, the metal distribution within the pellets of the support can be controlled by the preparation conditions. Several profile types can be established, like egg-shell (active component concentrated in the external area of the pellet), egg-yolk (metal concentrated in an internal region of the pellet) and uniform distribution. The establishment of an internal non-uniform profile can favorably influence the performance of the catalyst in many chemical processes. Several factors allow the control of the metal content and the profile of metal distribution, namely, impregnation time, pH, concentration of the impregnating solution, temperature and the use of additives.

The introduction and the fixation of the active phase in a catalytic support consist basically of transport and deposition of the material inside the pores of the support, drying and calcination. According to Vincent and Merril [1], for a cylindrical pore system with constant diameter and considering unidirectional plug-flow of the impregnation solution inside the pore, three phenomena can simultaneously occur: transport of the solution in the longitudinal direction of the pore, mass transfer in the liquid–solid interface and adsorption of the ions in the walls of the pores. The concentration profile will be defined by the relative weight of each phenomenon. Thus, if the adsorption is decisive in the process, there will be strong variation of solution concentration inside the pore. It causes a concentration gradient in the longitudinal direction of the pore that result in an egg-shell profile. When the adsorption forces are weak, ions distribution is more uniform in the interior of the pore and the metal concentration profile is more homogeneous.

Mathematical models of porous solids with different degrees of complexity and rigorousness have been reported, but the solution of the unsteady-state mass transport in a fluid flowing through tortuous channels of the actual pellet geometries would be a difficult task. For instance, Vincent and Merril [1], developed a model of a single cylindrical pore to analyze the time-dependence of liquid phase impregnation of a catalyst pellet. This model employs the plug-flow approximation considering the existence the of capillary, diffusion and adsorption forces, showing to be physically very reasonable. Morbidelli and Servida, [2], and Morbidelli and Varma [3], determined the optimal distribution

* Corresponding author. Tel.: +55-162739918; fax: +55-162739952.
E-mail addresses: eassaf@iqsc.sc.usp.br (E.M. Assaf), mansur@power.ufscar.br (J.M. Assaf).

1385-8947/03/$ – see front matter © 2003 Elsevier Science B.V. All rights reserved.
doi:10.1016/S1385-8947(03)00006-8

Nomenclature

c	impregnant concentration (mol/m^3)
c_0	impregnant initial concentration (mol/m^3)
c_s	areal adsorption capacity of the pore wall (mol/m^2)
c_w	concentration near the pore wall (mol/m^3)
d	axial coordinate in pore or radial coordinate in pellet (m)
D	diffusion coefficient (m^2/s)
k_m	mass transfer coefficient (m/s)
K	reduced mass transfer coefficient ($K = 2k_m t_L/R$)
K_L	constant of adsorption equilibrium (dimensionless)
K'_L	reduced equilibrium adsorption coefficient, ($K'_L = K_L/c_0$)
L	pore length (m)
P	pressure (N/m^2)
r	pore radius (m)
R	pellet radius or pore length (m)
t	time (s)
t_L	time for the solution to fill all the pores, (Eq. (6))
u	reduced velocity
v_p	penetration rate (m/s)
V	impregnant removal velocity (mol/(m^3 s))
z	radial position in pellet (m)

Greek letters

α	reduced diffusivity
Γ	reduced axial position in pore
η	relative capacity of adsorption ($\eta = 2c_s/rc_0$)
μ	viscosity (P)
θ	fractional covered
τ	reduced time
Ψ	reduced concentration

of catalyst within a pellet using analytical formulas as a function of the physicochemical parameters for some pellet geometries. Scelza et al. [4], presented a model based on diffusion–adsorption. The model describes the multicomponent impregnation of a porous support using limited quantities of each species. Competitive adsorption for some kind of adsorption sites with reversible kinetics was considered. Papageorgiou et al. [5], proposed the diffusion–adsorption model which predicts the catalyst distribution inside the pellet. The parameters of the model, adsorption constants and effective diffusivities were determined in separate experiments. Galarraga et al. [6], presented a methodology to produce egg-shell catalysts. It was demonstrated that parameters such as impregnation time, metal solution concentration, solution viscosity and state of support before impregnation, influence the evolution of the thickness and the final state of the metal in the egg-shell catalyst. Mathematical models were employed to describe both the dry impregnation and the wet impregnation. These models lead to reliable predictions of the formation of the egg-shell.

Several investigations have been reported about the non-homogeneous distribution of metallic catalysts in ceramic supports and the effect on the physical properties and reactivity of catalysts. Kunimori et al. [7], studied the performance of the alumina supported platinum catalyst in CO oxidation. They reported that the egg-yolk profile is more efficient than the egg-shell type to obtain multiple stationary states in the reaction and they attributed this to a smaller intrapellet diffusion resistance. Summers and Hegedus [8], reported the role of the palladium and platinum distribution on the performance and the life time of the catalyst in the oxidation of car exhaust gases. They concluded that the best catalyst was the one constituted by a platinum external layer and a palladium core. This distribution provided the highest sinterization and poison resistance of the catalyst. Mang et al. [9], reported that the metal distribution inside the alumina and silica pellets could be modified by changing the metallic salt solution and introducing competitive ions to the reactional medium. Iglesia et al. [10], reported the effect of the cobalt distribution on spherical silica supports applied to Fischer–Tropsch reaction synthesis. They concluded that the egg-shell profile provided better selectivity for C_5^+ compounds due to their smaller diffusional restrictions in the presence of CO. The silver profile in spherical pellets of alumina was studied by Prata et al. [11]. They reported that using high or low concentrations of solution and short or long contact times, uniform distributions were always obtained as a consequence of the weak adsorption force of Ag ions on the pore walls and by back-diffusion process at long impregnation times. The effect of the nature of the nickel salt was studied by Fujitani et al. [12]. They concluded that the starting source has a remarkable effect on both concentration profile and particle size of nickel supported on alumina spheres. The uses of nickel carbonates and nickel formate resulted in a uniform distribution, while nickel nitrate provided the formation of a remarkable egg-shell profile. The effect of post impregnation drying on nickel concentration profile in spherical alumina pellets was studied by Uemura et al. [13]. They concluded that the Ni segregation towards the outer surface of the support becomes significant with increasing post impregnation drying rate when nickel chloride aqueous solution is used.

Several important reactions, such as hydrogenation, dehydrogenation, partial oxidation and dry and steam reforming of hydrocarbons are catalyzed by nickel-on-alumina catalyst [14]. The catalyst efficiency is strongly affected by the preparation process. Thus, to obtain an active and selective catalyst, the preparation procedures should be controlled. The aim of this article is to report the results of an experimental study on the preparation and characterization of nickel-alumina catalysts, along with a mathematical model of the impregnation process that takes into account the diffusion and deposition of nickel inside the support, including

Table 1
Variables of the impregnation process

Variable	Values
Concentration (M)	0.01, 0.02, 0.04, 0.08, 0.10
Time (h)	0–24
Temperature (°C)	26, 60, 90

the dispersion of nickel in the interior of the pellet and its deposition into the pore walls.

2. Experimental procedure

2.1. Impregnation

Nickel-on-alumina catalysts were prepared by dry impregnation of gamma-alumina spheres (the porous solid was dried before being in contact with the impregnating solution) with a solution of nickel nitrate during a contact time at a given temperature. The 5-mm diameter pellets supplied by Degussa were pre-calcinated at 500 °C for 4 h under oxidizing atmosphere. After the impregnation, the catalyst was dried at 60 °C for 24 h and then calcinated at 600 °C for 5 h. The following variables were studied in the impregnation process: contact time, nickel concentration of the impregnating solution and temperature. The values of each variable are shown in Table 1.

2.2. Quantitative analysis of the radial distribution of nickel and observation of the nickel penetration depth

Nickel distribution profiles were measured by energy dispersive (X-ray) spectrometry (EDX) in a scanning electronic microscope (Zeiss). After impregnation and calcination, the pellets were sectioned and mechanically rubbed to expose the cross section, coated with a layer of carbon by vacuum deposition and submitted to quantitative microanalyses along the radial distances. In addition, in other pellets sectioned in the same way, an alcoholic solution of 10% dimetilglioxime was added to permit visual observation of the penetration depth. This surface was photographed and the penetration distances were measured.

3. Mathematical modeling of the impregnation process

Several mathematical models presented in literature may represent the transport and the deposition of the active phase in the pore walls of the catalytic pellet [1,13,15–17]. In the present study, a model proposed by Vincent and Merrill [1], based on cylindrical pore geometry, was applied to analyze the behavior of the system and to identify the most important parameters that determine the configuration of the concentration profile inside the pellet. In this model, the solution penetrates into the cylindrical pore by the action of capillary forces. As soon as it penetrates, the impregnant diffuses towards the walls and is removed from the solution by adsorption.

The hypotheses adopted to solve the mathematical model were based on the one-dimensional single-pore model with cylindrical geometry, concentration gradient only in the axial direction of the pore (i.e. radial gradients inside the pellet) and time-dependent plug-flow velocity of the penetrating liquid.

The partial-differential equation corresponding to mass balance is:

$$\frac{\partial c}{\partial t} + v_p \frac{\partial c}{\partial z} = D\frac{\partial^2 c}{\partial z^2} \tag{1}$$

The effect of the concentration gradient close to the pore wall is explained by the mechanisms of impregnant removal of the solution. Thus, a term describing the impregnating removal rate of the of the system $V(c, \theta)$ is added to Eq. (1):

$$\frac{\partial c}{\partial t} + v_p \frac{\partial c}{\partial z} = D\frac{\partial^2 c}{\partial z^2} + V(c, \theta) \tag{2}$$

To adimensionalize Eq. (2), the following definitions are used:

$$\Gamma = \frac{z}{L}, \quad \psi = \frac{c}{c_0}, \quad \tau = \frac{t}{t_L}, \quad \alpha = \frac{Dt_L}{L^2}, \quad u = \frac{v_p t_L}{L}$$

obtaining:

$$\frac{\partial \Psi}{\partial \tau} + u\frac{\partial \Psi}{\partial \Gamma} = \alpha\frac{\partial^2 \Psi}{\partial \Gamma^2} + \frac{t_L}{c_0} V(c_0\Psi, \theta)\Lambda \tag{3}$$

In practical situations, where the diffusivity value is much shorter than the unity, α is also much shorter than the unity. The $(t_L/c_0)V$ represents the relationship between the impregnant removal at the pore wall and the impregnation concentration and can be approximated by ΨK. Considering $K \sim 1$, the first term on the right side of Eq. (3) can be neglected. Then the mass balance becomes:

$$\frac{\partial \Psi}{\partial \tau} + u\frac{\partial \Psi}{\partial \Gamma} = \frac{t_L}{c_0} V(c_0\Psi, \theta) \tag{4}$$

with:

$$\Psi(0, \tau) = 1 \quad \text{and} \quad \Psi(0, 0) = 1$$

The impregnating solution penetration rate and the pore filling time are:

$$v_p = \frac{r}{4}\left(\frac{\Delta P}{\mu}\right)^{1/2} t^{1/2} \tag{5}$$

$$t_L = \frac{4L\mu}{r^2 \Delta P} \tag{6}$$

The mechanism of impregnant removal at pore walls can be controlled by mass transfer or by adsorption kinetics. Vincent and Merril [1], have shown that both mechanisms show

similar results. In this work the mechanism of impregnant removal controlled by mass transfer was adopted:

$$V = \frac{-2k_m}{r}(c - c_w) \tag{7}$$

With Eqs. (5)–(7) and considering

$$\frac{\partial(\theta c_s)}{\partial t} = k_m(c - c_w) \tag{8}$$

where,

$$\theta = \frac{K'_L c_w}{1 + K'_L c_w}$$

obtaining:

$$\frac{\partial \Psi}{\partial \tau} + \frac{1}{2\tau^{1/2}}\frac{\partial \Psi}{\partial \Gamma} = -K\left(\Psi - \frac{\theta}{K_L(1-\theta)}\right) \tag{9}$$

$$\frac{\partial \theta}{\partial \tau} = \frac{K}{\eta}\left(\Psi - \frac{\theta}{K_L(1-\theta)}\right) \tag{10}$$

where,

$$K = \frac{2k_m t_L}{r}, \quad \eta = \frac{2c_s}{rc_0}, \quad K_L = K'_L c_0$$

The existence of three variables that describe the impregnation process is observed: K, reduced mass transfer coefficient; η, relative capacity of adsorption of the pore wall and K_L, adsorption equilibrium constant.

4. Results and discussion

4.1. Visual observation of the penetration distance of nickel on the support

The visual observation showed that the penetration distance of the active phase was influenced by the concentration of the impregnating solution, time of contact and temperature. By increasing the concentration of the impregnating solution, the penetrated distance is more extensive. The effect of temperature variation is less significant otherwise. The results of the influence of the contact time on the penetration distance showed that the higher the concentration of the solution, the smaller the necessary time to reach the center of the pellet. As an example, Fig. 1 shows the influence of the contact time on the penetration distance for a 0.1 M concentration. On the other hand, for the diluted solutions the time necessary to achieve the equivalent penetration distance is high.

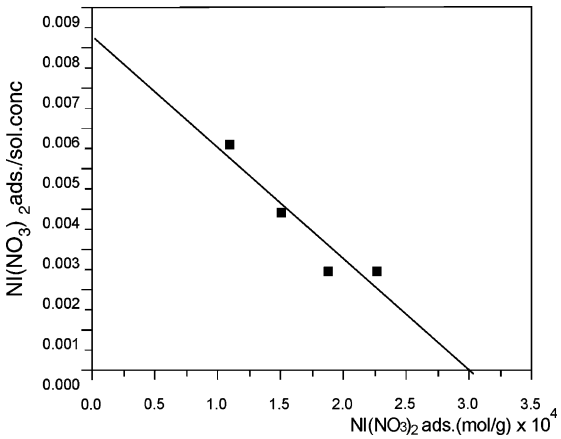

Fig. 2. Isotherm of adsorption.

4.2. Quantitative analysis of the profiles and mathematical models

The adsorption capacity of the pore wall for unit of area (c_s) and the reduced equilibrium adsorption coefficient ($K'_L = K_L/c_0$) are determined from the slope of the straight line shown in Fig. 2 which represents a Langmuir isotherm. The experimental values represented in this illustration were obtained elsewhere Jesus and Assaf [18].

According to Komiyama et al. [15], the value of K'_L is given by the module of the value of the slope of the straight line. The c_s value is given by the inverse of the angular coefficient multiplied by the specific area and divided by the specific pore volume of the support.

The reduced mass transfer coefficient (K) is obtained by the adjustment of the simulation curves of the impregnation process to the EDX experimental points. K_L and η values were experimentally determined and K was obtained by this adjustment. Table 2 shows the values of these parameters.

Figs. 3 and 4 show a comparison between model predictions (continuous line) and the experimental data (points), obtained by the EDX analysis, for the nickel concentration along the radial distance in the pellet. Fig. 5 shows the

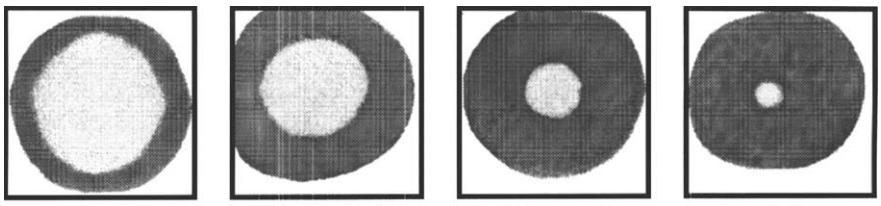

Fig. 1. Photographs of the surface of the sectioned pellets, showing the impregnation front as function of time (impregnating solution concentration 0.10 M): (a) 15 min; (b) 60 min; (c) 135 min; (d) 195 min.

Table 2
Parameters obtained experimentally (K'_L = 25.32, c_s = 8.58 × 10^{-8} mol/m^2)

Solution concentration (M)	η	K_L	K
0.02	1.97	0.51	Very high
0.04	0.98	1.01	10.0
0.10	0.39	2.53	0.4

experimental data obtained when the temperature was varied. The partial-differential equations that describe the concentration profiles of the impregnant and the fractional coverage on the pore walls (Eqs. (9) and (10)), was numerically solved using backward finite-difference formulas to discretize the space variable (radial position in the pellet), and integrating the resulting set of ordinary-differential equations in time with a marching algorithm standard (an explicit Runge–Kutta method with variable step). As observed in Figs. 3 and 4, satisfactory agreement was achieved, revealing that the simplifications assumed in the model are sound under the experimental conditions studied. On the other hand the effect of the impregnation temperature is less significant.

4.3. Model parameters analysis

The K'_L and K values were varied in 50% to analyze the influence of these parameters on the nickel distribution profile, i.e. the parametric sensitivity of the mathematical model. Figs. 6 and 7 show the results of these simulations. As seen in Fig. 6, for diluted solution (0.04 M), K_L influences only the saturation degree (θ), interfering only a little in the penetration depth in the pellet radial direction and in the extension of the saturated area (length of the region of constant concentration). The increase of K_L value in solutions with high η and K values favors the removal of the impregnant

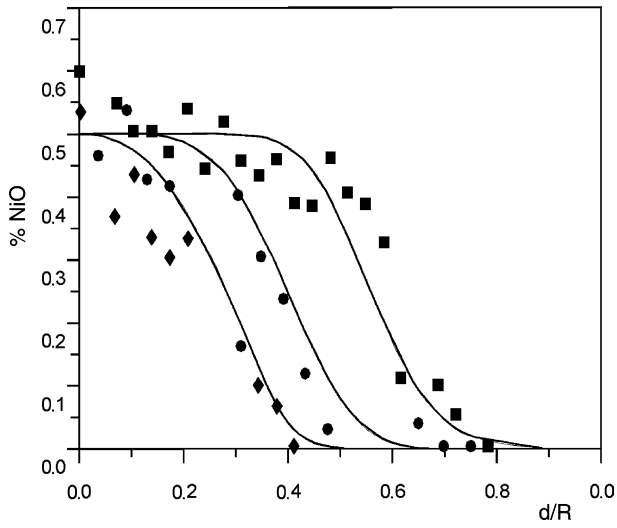

Fig. 4. Experimental and theoretical profiles for the concentration 0.04 M: (◆) 3 h; (●) 6 h; (■) 12 h.

of the solution. For more concentrated solutions, other simulation results showed that the effect of K_L is also limited to the saturation degree. In this case, when the solution/pore wall mass transfer resistance is high (low values of K), the formation of a well-delineated constant concentration region does not occur.

Fig. 7 shows the effect of the variation of the solution/wall mass transfer parameter K on the nickel concentration profile. Although not shown here, it was also observed that for more concentrated solutions (0.10 M), low values of K influence on the saturation degree, as the mass transfer is drastically reduced and, as a consequence, most of the nickel remains in solution. For the highest K values (0.6–1.2) the degree of coverage does not change, but there is an increase in the region of constant concentration. In this sit-

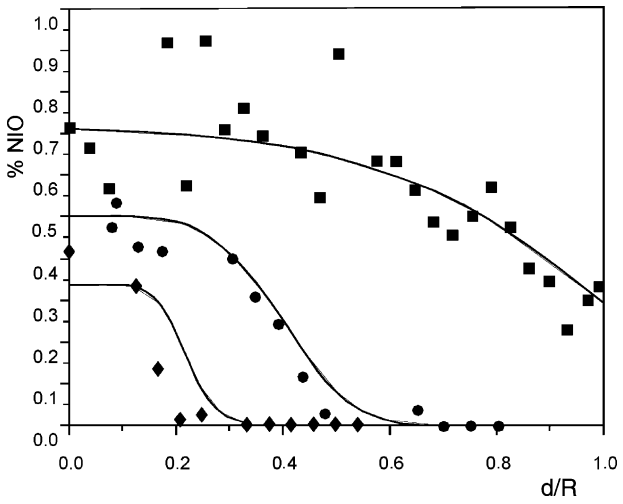

Fig. 3. Experimental and theoretical profiles in 6 h of contact for the concentrations: (◆) 0.02 M; (●) 0.04 M; (■) 0.10 M.

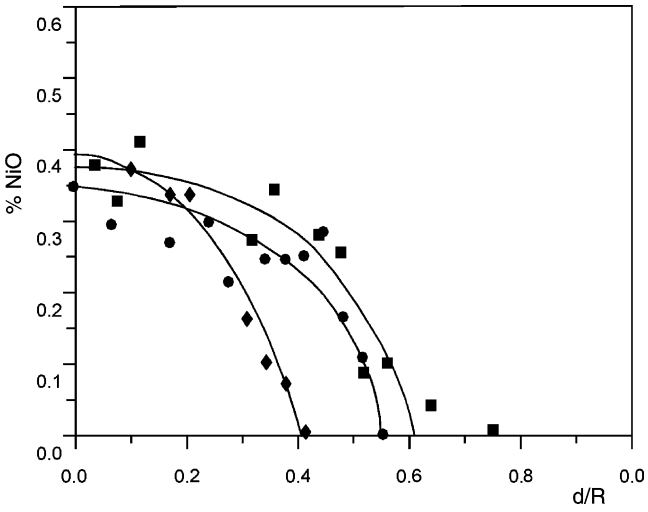

Fig. 5. Experimental data for the concentration 0.04 M: (◆) 26 °C; (●) 60 °C; (■) 90 °C.

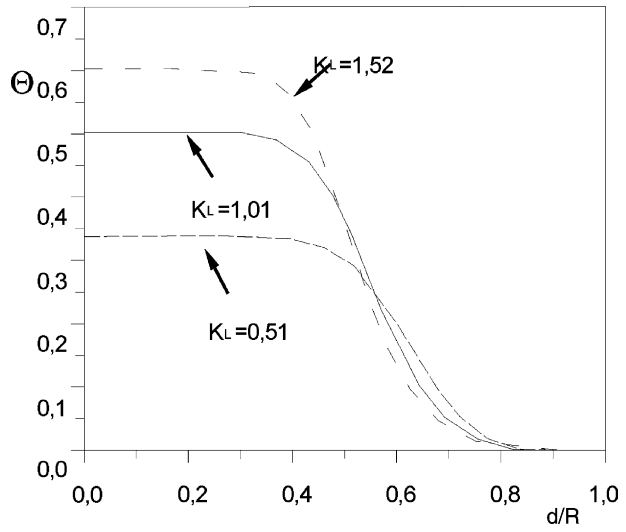

Fig. 6. Distribution profiles formed by the variation of ±50% of the parameter K_L. $C = 0.04$ M, $K = 10$, $\eta = 0.98$.

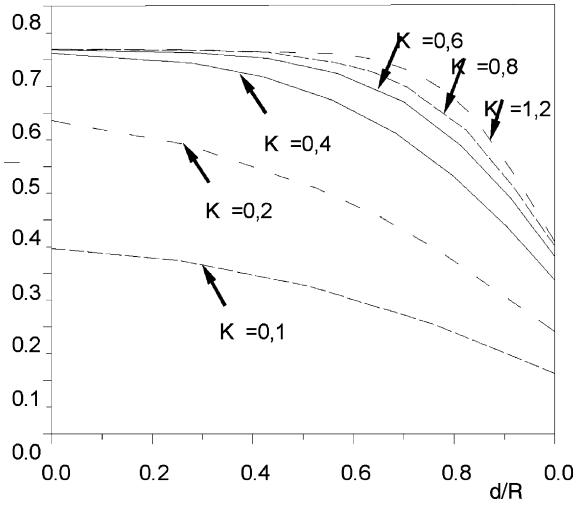

Fig. 7. Distribution profiles formed by the variation of the parameter K. $C = 0.10$ M, $K_L = 2.53$, $\eta = 0.39$.

uation, the mass transfer is sufficiently large and the wall reaches its maximum saturation degree. For diluted solutions, simulations showed that a variation in K value results in a small influence on the nickel concentration profiles. The mass transfer to the pore wall increases and only a small amount of available nickel is remained to diffuse inside the pore.

5. Conclusions

The impregnation solution concentration is the parameter that establishes the degree of recoverage and the penetrated distance by he nickel inside the catalytic pore at a certain impregnation time. By increasing the solution concentration, a larger degree of coverage was obtained and the necessary time to reach a given axial distance is smaller. The effect of impregnation temperature is less significant.

The non-homogeneous nickel distributions along the radial position of the pellet indicate that the mass transfer and/or adsorption coefficients are high and that the process is limited by the solution penetration velocity and/or by the solute diffusion velocity in the axial direction of the pore.

Through a comparison between the mathematical model that represents the impregnation process and the experimental data, a satisfactory agreement was achieved, revealing that the simplifications assumed are sound under the experimental conditions studied. The model can be employed as a useful tool to design spatial nickels profiles in the pellet.

References

[1] R.C. Vincent, R.P. Merril, J. Catal. 35 (1974) 206–217.
[2] M. Morbidelli, A. Servida, Ind. Eng. Chem. Fundam. 21 (1982) 278–284.
[3] M. Morbidelli, A. Varma, Ind. Eng. Chem. Fundam. 21 (1982) 284–289.
[4] O.A. Scelza, A.A. Castro, D.R. Ardiles, J.M. Parera, Ind. Eng. Chem. Fundam. 25 (1986) 84–88.
[5] P. Papageorgiou, D.M. Price, A. Gavriilidis, A. Varma, J. Catal. 158 (1996) 439–451.
[6] C. Galarraga, E. Peluso, H. Lasa, Chem. Eng. J. 82 (2001) 13–20.
[7] K.K. Kunimori, E. Kawasaki, I. Nakajima, I.E. Uchijima, Appl. Catal. 22 (1986) 115.
[8] J.C. Summers, L.L. Hegedus, J. Catal. 51 (1978) 185.
[9] T. Mang, B. Breitscheidel, P. Polanek, H. Knozinger, Appl. Catal. 106 (1993) 239.
[10] E. Iglesia, S.L. Soled, J.E. Baumgartner, S.C. Reyes, J. Catal. 153 (1995) 108.
[11] A.S. Prata, E.M. Assaf, J.M. Assaf, Adsorption'98—II Brazilian Congress of Adsorption, Florianópolis, Brazil, 1998, pp. 131–137.
[12] T. Fujitani, O. Ueki, E. Echigoya, Bull. Chem. Soc. Jpn. 62 (1989) 2753.
[13] Y. Uemura, Y. Hatate, A. Ikari, J. Chem. Eng. Jpn. 20 (2) (1987) 117–123.
[14] M.A. Pena, J.P. Gómez, J.L.G. Fierro, Appl. Catal. 144 (1996) 7.
[15] M. Komiyama, R.P. Merril, A.F. Harnsberger, J. Catal. 63 (1980) 35–52.
[16] M.S. Heise, J.A. Schwarz, J. Colloid Interf. Sci. 123 (1) (1988) 51–58.
[17] P. Chu, E.E. Petersen, C.J. Radke, J. Catal. 117 (1989) 52–70.
[18] L.C. Jesus, J.M. Assaf, Brazilian Congress of Chemical Engineering, vol. 2, São Paulo, 1998, pp. 1006–1010.